06,13

The influence of the PZT buffer layer on electrophysical properties of MDM structures with the BST film

© *M.S. Afanasiev*[1], *D.A. Belorusov*[1], *D.A. Kiselev*[1,2], *A.A. Sivov*[1], *G.V. Chucheva*[1,¶]

[1] Fryazino Branch, Kotel'nikov Institute of Radio Engineering and Electronics, Russian Academy of Sciences, Fryazino, Moscow oblast, Russia
[2] National University of Science and Technology „MISiS",
Moscow, Russia

[¶] E-mail: gvc@ms.ire.rssi.ru

Received July 5, 2021
Revised July 5, 2021
Accepted July 7, 2021

Films of the composition $Ba_{0.8}Sr_{0.2}TiO_3$ (BST) were synthesized by the method of high-frequency (HF) sputtering on the buffer layer of a ferroelectric film of the composition $PbZr_xTi_{1-x}O_3$ (PZT). Comparative results of electrophysical properties of three different metal–dielectric–metal (MDM)-structures are presented: Pt/BST/Ni, Pt/PZT/Ni, and Pt/PZT-BST/Ni.

Keywords: metal–dielectric–metal structures, ferroelectric films of composition $Ba_{0.8}Sr_{0.2}TiO_3$, a buffer layer, electrophysical properties.

DOI: 10.21883/PSS.2022.13.52318.161

1. Introduction

Ferroelectric thin-film materials, including multilayer materials, are widely used as active elements in tunable microwave devices, piezoelectric drives, sensors, microelectromechanical systems (MEMS), in elements of static and dynamic memory with high information density and high speed. The most promising ferroelectric materials for these applications are compositions based on lead zirconate titanate ($PbZrTiO_3$ or PZT) and barium strontium titanate ($Ba_{1-x}Sr_xTiO_3$ or BST) [1–6]. Thus, BST thin films have been studied in detail as potential materials for the above applications due to their high dielectric permittivity, relatively low dielectric loss tangent, long service life and good temperature stability [7–9]. It becomes possible to control the level of dielectric nonlinearity and temperature properties of the film, as well as the figure of merit of the ferroelectric heterostructure based on BST, due to the variation in Ba/Sr concentration ratio, that specifies the temperature of the phase transition from ferroelectric to paraelectric phase and thus the operating temperature range. For example, the use of ferroelectric films of the compositions $Ba_{0.67}Sr_{0.33}TiO_3$ [10] and $Ba_{0.55}Sr_{0.45}TiO_3$ [11] in periodic multilayer structures opens up the possibility of creating capacitors with the prospect of their practical application in modern microelectronics. The study [12] shows that due to the variation of $Ba_{0.2}Sr_{0.8}TiO_3$ sublayer thickness and/or the amplitude of one period of the external bipolar field action it is possible to create various electrophysical states of the structure, and this can serve as basis for creating a memory cell, in particular, a multilevel one. In the studies [13–15] the optimal Zr/Ti ratios were determined, where the ferroelectric properties of the films are mostly apparent. The main problem of creating PZT is a high lead volatility during the film formation. The combined use of BST and PZT films in one heterostructure will possibly provide a significant gain in active elements and MEMS sensitivity at minimal engineering costs. This study presents the results of studying three different heterostructures metal–ferroelectric–metal (MDM) Pt/BST/Ni, Pt/PZT/Ni and Pt/PZT-BST/Ni.

2. Technology of obtaining MDM structures and experiment procedure

For the studies heterostructures which include a silicon substrate with a platinum electrode, a buffer layer made of a PZT ferroelectric film, $Ba_{0.8}Sr_{0.2}TiO_3$ ferroelectric film and an upper nickel electrode were formed, as well as structures tPt/BST/Ni, Pt/PZT/Ni.

A ferroelectric film $Ba_{0.8}Sr_{0.2}TiO_3$ (BST) was deposited by HF spraying on Plasma-50SE unit [16] on a previously deposited buffer ferroelectric PZT film layer. Process parameters of deposition: substrate temperature 620°C; oxygen pressure 0.5 Torr, target–substrate distance 10 mm.

The upper nickel electrode was formed onto a BST film using electron beam method through a shadow mask on the A700QE/DI12000 unit, Germany. Process parameters of deposition: structure temperature 70°C; deposition speed 2.0 A/s. Electrode area $2.7 \cdot 10^{-4}$ cm^2, thickness 0.1 μm.

To determine the structure thickness, Nova NanoSEM 230 scanning electron microscope (SEM) by FEI was used.

The electrophysical properties of the obtained heterostructures were studied on the measuring bench described in the studies [17–18].

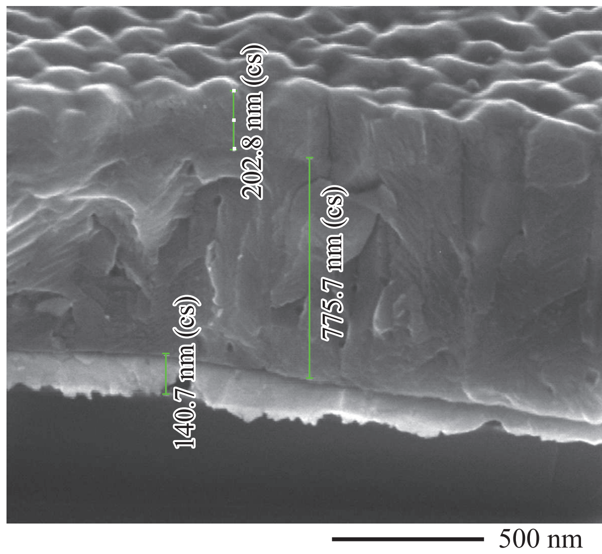

Figure 1. SEM image of Pt/PZT-BST/Ni heterostructure sheared surface.

Scanning probe microscopy studies were performed using Ntegra Prima nanolaboratory (NT-MDT SI, Russia) in piezoresponse force microscopy (PFM) mode using NSG10/Pt cantilever (Tipsnano, Tallinn, Estonia).

3. Results and discussions

Fig. 1 demonstrates SEM image of Pt/PZT-BST/Ni heterostructure sheared surface.

SEM image of Pt/PZT-BST/Ni heterostructure sheared surface showed that the thickness of Pt electrode was 140 ± 10 nm, of PZT film — 770 ± 10 nm, of BST film — 200 ± 10 nm.

Fig. 2 demonstrates volt-farad characteristics (VFCs) of three heterostructures Pt/BST/Ni, Pt/PZT/Ni and Pt/PZT-BST/Ni, measured at room temperature at a frequency of 100 kHz and a measurement signal amplitude of 25 mV. The dependences of heterostructure C capacitance on the electrical bias V_g, varying from -20 to $+20$ V (forward stroke) and from $+20$ to -20 V (return stroke)

Figure 2. VFCs of MDM structures with ferroelectric layer composition: *a*) BST, *b*) PZT, *c*) multilayer BST-PZT ($f = 100$ kHz).

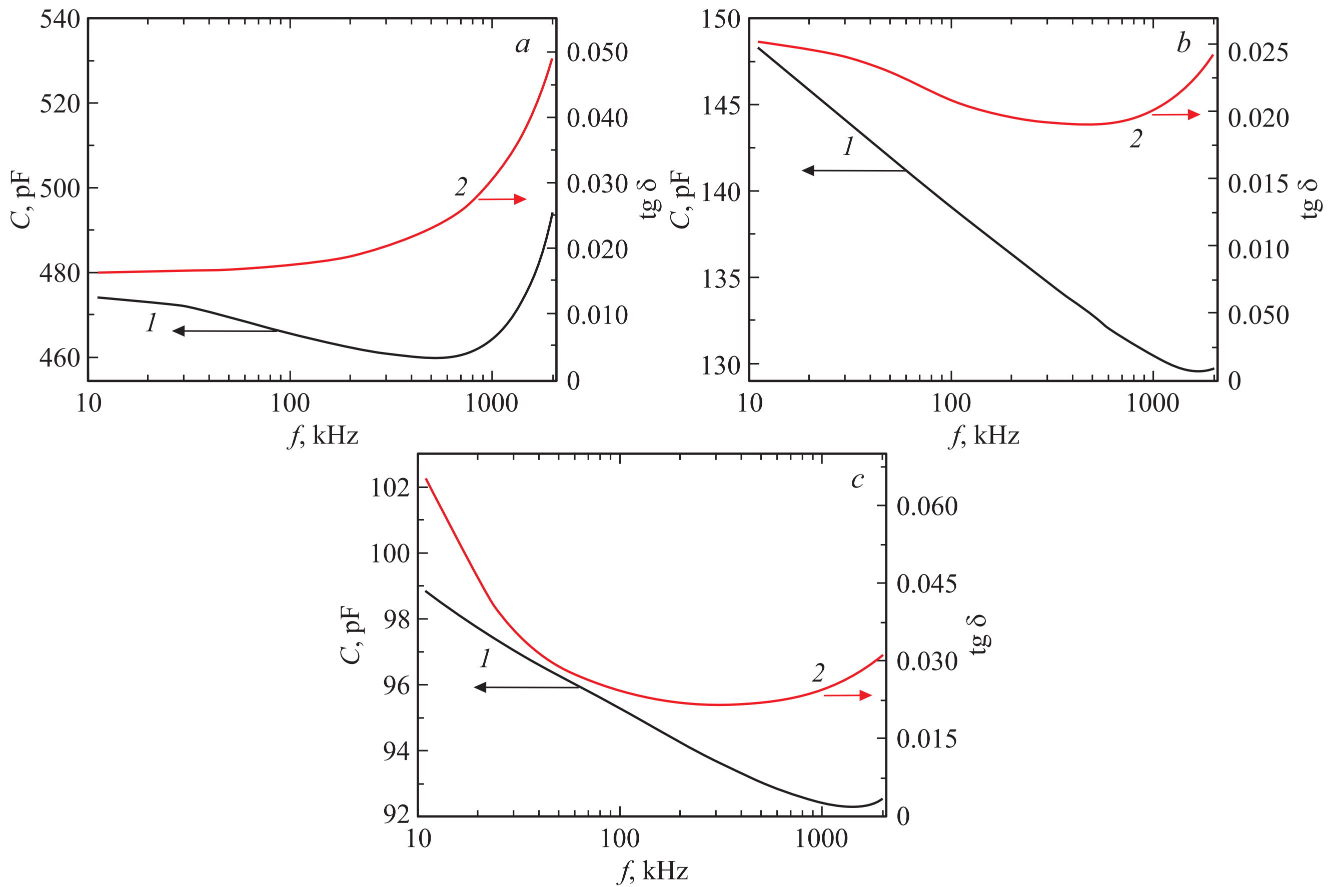

Figure 3. Dependences of C capacitance (curves *1*) and dielectric loss tangent $\operatorname{tg}\delta$ (curves *2*) on the frequency for MDM structures with ferroelectric layer composition: *a*) BST, *b*) PZT, *c*) BST-PZT multilayer.

with a discretion of 5 mV and instrument reading speed of 3 point/s, were recorded.

The dependence of capacitance on electrical bias for Pt/BST/Ni and Pt/PZT-BST/Ni samples has a typical bell shape. VFC curves shapes for Pt/PZT-BST/Ni heterostructure, corresponding to the forward and return strokes, are more similar to each other than for Pt/BST/Ni object. This allows us to speak of a more stable Pt/PZT-BST/Ni structure behavior.

Pt/BST/Ni heterostructure is characterized by a higher capacitance value compared to Pt/PZT/Ni and Pt/PZT-BST/Ni samples.

The maximum capacitance value for the Pt/PZT/Ni structure was observed at $V_g \approx 15.0$ V. The shift of the maximum relative to the point $V_g = 0$ V may be due to the presence of a built-in charge in the ferroelectric film and the charge caused by both structural defects in PZT and surface states on interphase boundaries.

The ratio of the maximum sample capacitance to the minimum capacitance was Pt/BST/Ni — 1.98, Pt/PZT/Ni — 1.42 and Pt/PZT-BST/Ni — 1.12.

Fig. 3 demonstrates the measured at room temperature and constant voltage ($V_g = \text{const}$) frequency dependences of C capacitance and dielectric loss tangent $\operatorname{tg}\delta$ of heterostructures Pt/BST/Ni, Pt/PZT/Ni and Pt/PZT-BST/Ni. The value V_g corresponds to the maximum capacitance $C_{\max}$ taken from VFCs for Pt/BST/Ni $V_g = -0.6$ V, for Pt/PZT/Ni $V_g = 13$ V for Pt/PZT-BST/Ni $V_g = 5$ V (Fig. 2).

As far as frequency grows, Pt/BST/Ni heterostructure capacitance grows, and Pt/PZT/Ni structure capacitance falls down within the frequency range 0.2–2.0 MHz. It should be noted that capacitance value versus frequency for Pt/PZT-BST/Ni heterostructure falls down within the frequency range 10–1.0 MHz and practically does not change within the frequency range 1.0–2.0 MHz. This fact allows us to say that Pt/PZT-BST/Ni samples are more stable in frequency.

The dielectric loss tangent for Pt/PZT/Ni and Pt/BST/Ni heterostructures grows with the growth of frequency. For Pt/PZT-BST/Ni structures the dielectric loss tangent practically does not change in the frequency range 0.2–2.0 MHz and is 0.025–0.032.

Fig. 4 demonstrates the dependences of capacitance and dielectric loss tangent of Pt/PZT-BST/Ni heterostructure on temperature and switching cycles at electrical bias equal to 5 V and frequency 100 kHz.

It is shown that the capacitance and dielectric loss tangent increase linearly within the temperature range25-115°C and

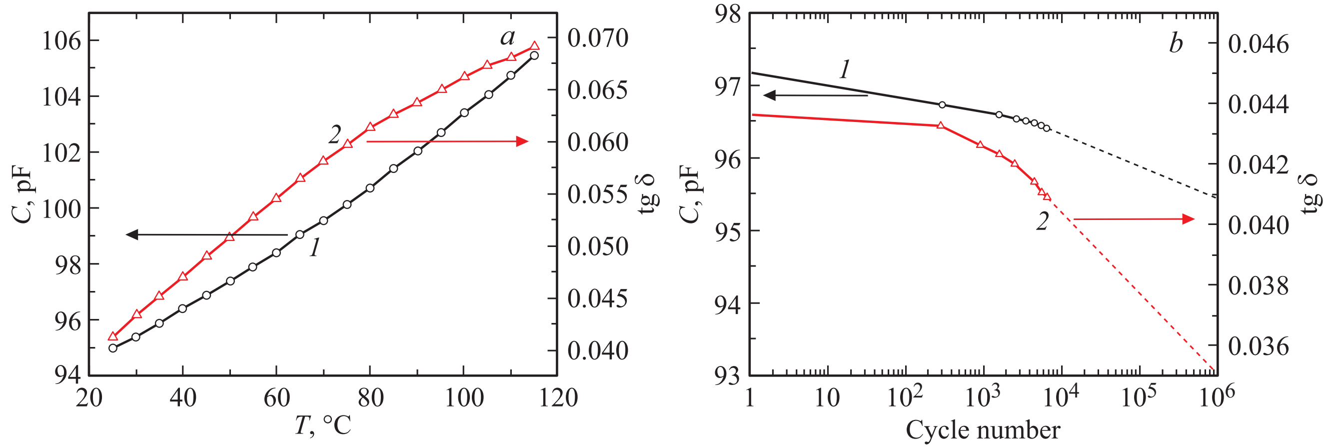

Figure 4. Dependences capacitance C (curves *1*) and dielectric loss tangent $\mathrm{tg}\,\delta$ (curves *2*) of Pt/PZT-BST/Ni heterostructure on: *a*) temperature and *b*) switching cycles.

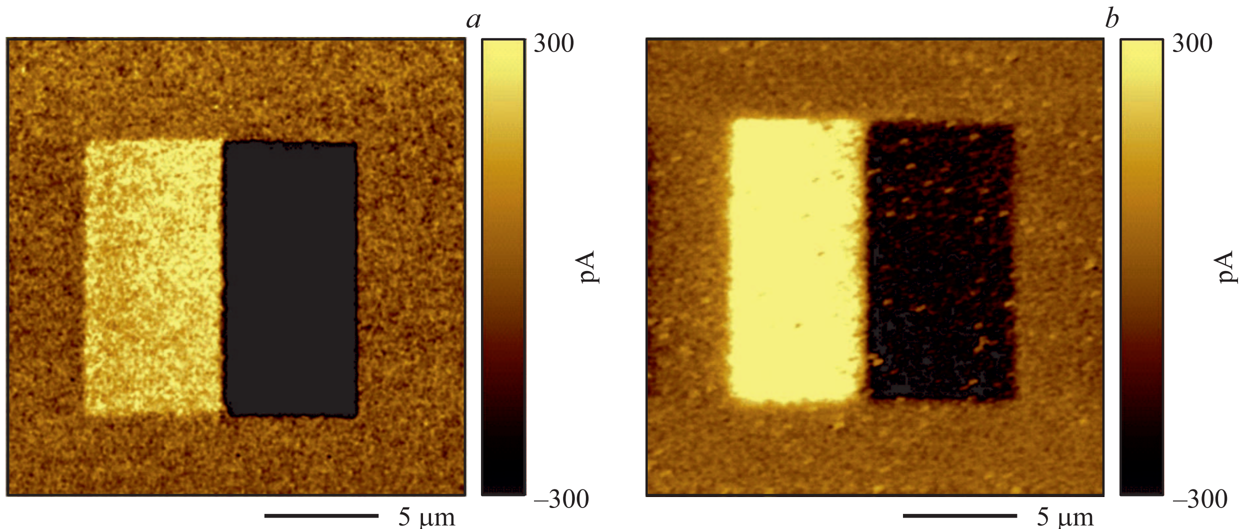

Figure 5. Signal of PZT film (*a*) and multilayer BST-PZT (*b*) piezoelectric response after polarization (light area +25 V, dark area: −25 V).

equals at 20°C to 95 pF and 0.04, and at 115°C to 105 pF and 0.07 correspondingly.

It is shown that after 10^4 switching cycles of the Pt/PZT-BST/Ni heterostructure, the capacitance values practically did not change. The values of dielectric loss tangent of Pt/PZT-BST/Ni sample do not change up to $5 \cdot 10^2$ cycles and change, but not more than by 10% within the range from $5 \cdot 10^2 \rightarrow 10^4$ cycles. It is planned to carry out further studies of Pt/PZT-BST/Ni heterostructure with the number of switching cycles exceeding 10^4. The results will be presented in future studies.

Fig. 5 demonstrates the signals of residual piezoelectric response of PZT film (Fig. 5, *a*) and BST-PZT multilayer (Fig. 5, *b*) after polarization with constant voltage ±25 V, supplied to the scanning probe microscope cantilever (upper electrode). The images clearly show polarized regions corresponding to different polarization directions: „light“ — from film surface to substrate, „dark“ — to film surface. In addition, it was found, that in the samples under study the piezoelectric response signal in the induced areas has different intensity (amplitude) (Fig. 6).

For example, in the case with PZT film the amplitude of the piezoresponse signal for the area polarized with negative voltage is 2 times higher than the signal for the area polarized with positive voltage (Fig. 6, curve *1*).

For BST-PZT multilayer, the opposite picture is observed — Fig. 6, curve *2*. Earlier in the study [16], according to the results of residual potential visualization it was shown, that in BST film synthesized on a platinized silicon substrate, an asymmetric signal is also observed between positive and negative polarized areas.

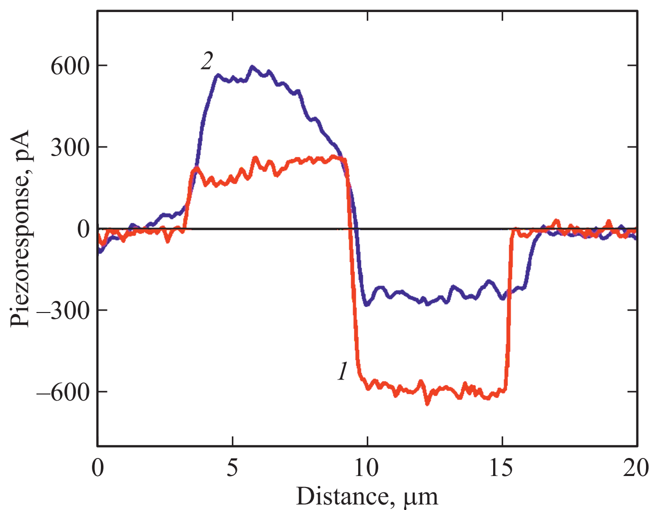

Figure 6. Piezoelectric response signal profiles drawn in the middle of the scans shown in Fig. 5. *1* — PZT film, *2* — BST-PZT multilayer.

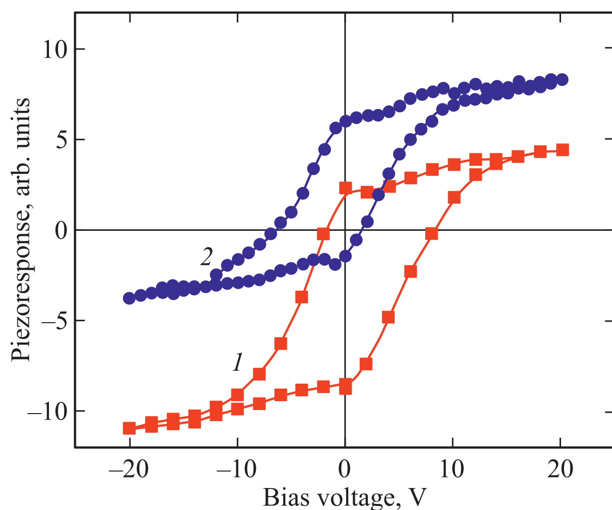

Figure 7. Residual piezoelectric hysteresis loops: *1* — PZT film, *2* — BST-PZT multilayer.

Fig. 7 demonstrates the residual piezoelectric hysteresis loops obtained under the same experimental conditions. As in the case of „macroscopic" polarization (Fig. 6), a similar asymmetry of polarization switching is observed for the structures under study: PZT film is characterized by a negative *imprint* — shift of the hysteresis loop towards positive voltages and a smaller value of the positive signal of the residual piezoresponse in comparison with the negative one (Fig. 7 curve *1*), for PZT-BST multilayer — positive.

A difference is also observed in the effective switching operation, that is defined as the area of hysteresis loop: for the PZT film, the area was 120 rel. units, for PZT-BST multilayer $S = 77$ rel. units, this makes the latter more ferro-soft material in comparison with „clean" PZT film.

4. Conclusion

The performed studies have shown the influence of PZT buffer layer on dielectric characteristics of MDM structures based on ferroelectric BST films. It turned out that Pt/PZT-BST/Ni heterostructures have a more stable frequency dependence in comparison with the Pt/PZT/Ni and Pt/BST/Ni samples. And in Pt/PZT-BST/Ni heterostructure an insignificant decrease in the ratio of the maximum sample capacitance to the minimum one comparing to Pt/BST/Ni structure is observed. The results of force microscopy of piezoelectric response of the structures under study revealed an asymmetry of the residual polarization signal, that is associated with the presence of an internal field, the magnitude and direction of which, in its turn, depends on buffer ferroelectric layer material in MDM structures under study.

Work funding

This study was carried out within the framework of a state assignment and partially supported by the Russian Foundation for Basic Research (RFBR projects No. 18-29-11029, No. 19-07-00271 and No. 19-29-03042).

Conflict of interest

The authors declare that they have no conflict of interest.

References

[1] B. Piekarski, M. Dubey, D. De Voe, E. Zakar, R. Zeto, J. Conrad, R. Piekarz, M. Ervin. Integrated Ferroelectrics **24**, 147 (1999).
[2] E. Zakar, M. Dubey, B. Piekarski, J. Conrad, R. Piekarz, R.J. Widuta. Vac. Sci. Technol. **19**, *1*, 345 (2001).
[3] S. Gevorgian. Ferroelectrics in Microwave Devices. Circuits and Systems. Springer, N.Y. (2009). 365 p.
[4] N. Setter, D. Damjanovic, L. Eng, G. Fox, S. Gevorgian, S. Hong, A. Kingon, H. Kohlstedt, N.Y. Park, G.B. Stephenson, I. Stolitchnov, A.K. Taganstev, D.V. Taylor, T. Yamada, S. Streiffer. J. Appl. Phys. **100**, 051606 (2006).
[5] F.-C. Sun, M.T. Kesim, Y. Espinal, S.P. Alpay. J. Mater. Sci. **51**, 499 (2016).
[6] L.W. Martin, A.M. Rappe. Nature Rev. Mater. **2**, 16087 (2017).
[7] C.L. Chen, J. Shen, S.Y. Chen, G.P. Luo, C.W. Chu, F.A. Miranda, F.W. Van Keuls, J.C. Jiang, E.I. Meletis, H.Y. Chang. Appl. Phys. Lett. **78**, 652 (2001).
[8] T. Kawakubo, S. Komatsu, K. Abe, K. Sano, N. Yanase, N. Fukushima. Jpn. J. Appl. Phys. **37**, 5108 (1998).
[9] J. Vukmirović, A. Nesterović, I. Stijepović, M. Milanović, N. Omerović, B. Bajac, J. Bobić, V.V. Srdić. J. Mater. Sci. Mater. Electron. **30**, 14995 (2019).
[10] X.Y. Chen, Z.P. Xu, D.X. Yan, Y.S. Fan, J.G. Zhu, P. Yu. J. Alloys Compd. **695**, 1913 (2017).

[11] P. Gardes, M. Diatta, M. Proust, E. Bouyssou, P. Poveda. J. Appl. Phys. **129**, 214101 (2021).
[12] S.P. Zinchenko, D.V. Stryukov, A.V. Pavlenko, V.M. Mukhortov. ZhTF (in Russian) **46**, 41 (2020).
[13] C.-S. Park, S.-M. Lee, H.-E. Kim. J. Am. Cer. Soc. **90**, *9*, 2923 (2008).
[14] M. Layns, A. Glass. Segnetoelektriki i rodstvennye materialy (in Russian) / Edited by V.V. Lemanov, G.A. Smolensky. Mir, M. (1981). 736 p.
[15] B.A. Tuttle, R.W. Schwartz. MRS Bull. **21**, *6*, 49 (1996).
[16] M.S. Afanas'ev, D.A. Kiselev, S.A. Levashov, V.A. Luzanov, A. Nabiev, V.G. Naryshkina, A.A. Sivov, G.V. Chucheva. FTT (in Russian) **60**, *5*, 951 (2018).
[17] E.I. Gol'dman, A.G. Zhdan, G.V. Chucheva. PTE (in Russian) **6**, 110 (1997).